

1. Supplemental figures:

Supplemental 15

Supplemental Figure1

Supplemental Figure2

Supplemental Figure3

Supplemental Figure4

Supplemental Figure5

Supplemental Figure6

Supplemental Figure7

Supplemental Figure8

Supplemental Figure9

Supplemental Figure10

Supplemental Figure11

Supplemental Figure12

Supplemental Figure13

Supplemental Figure14

2. Supplemental tables:

Supplemental Table1

Supplemental Table2

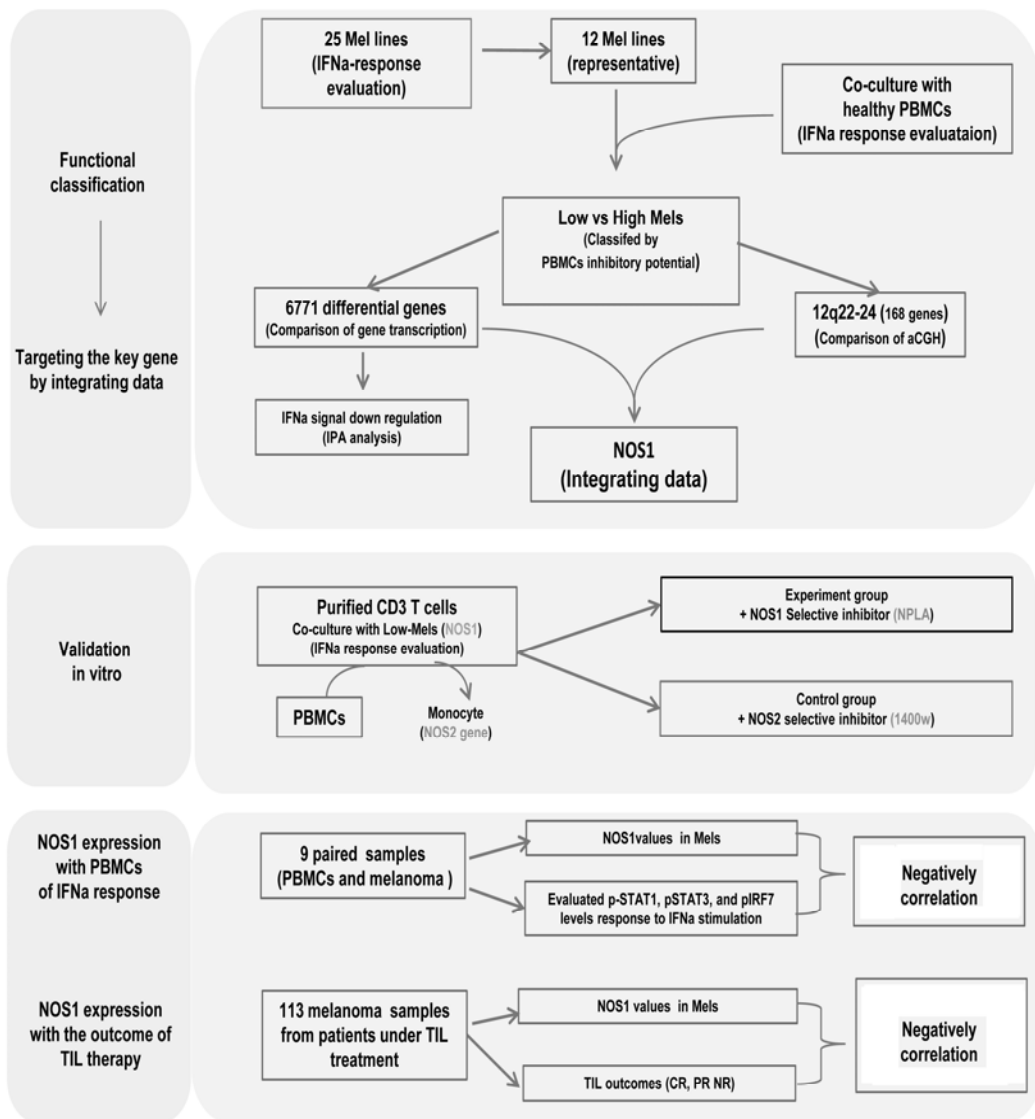
Supplemental Table3

Supplemental Table4

3. Supplemental Methods:

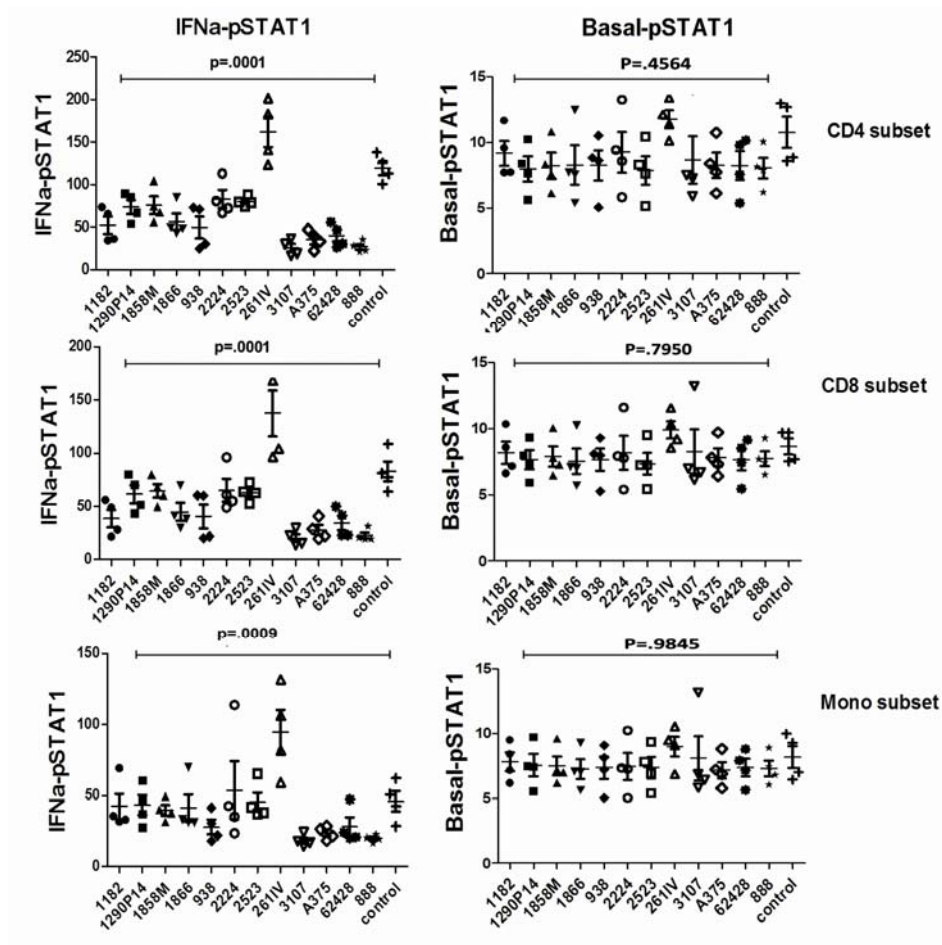
Patients and samples used for in vivo analysis of melanoma metastases.

1. Supplemental Figures:



Supplemental Figure15: Study Workflow

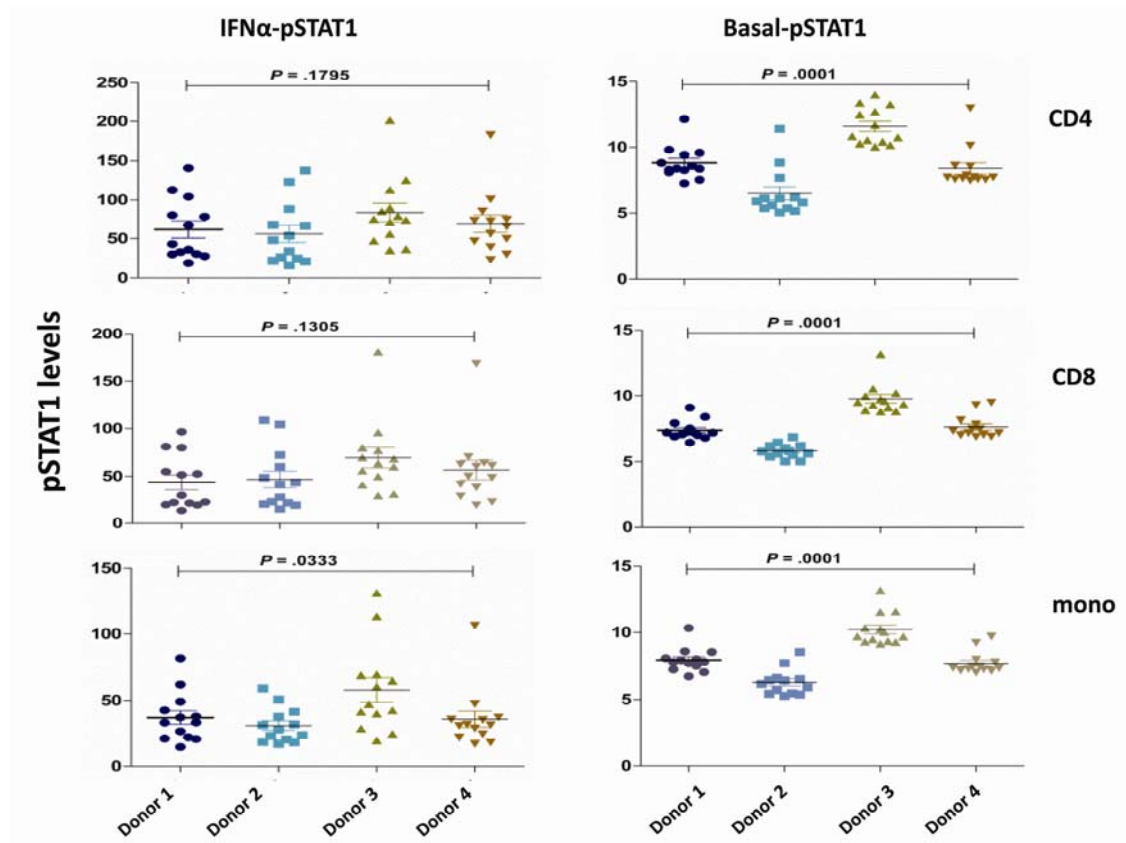
Top panel: Integrating analysis of immune inhibitory melanoma-cells (Low-Mels) compared to non-inhibitory melanoma-cells (High-Mels). 12 melanoma cell lines selected from 25 lines representative of heterogeneity in IFN- α -pSTAT1 levels were co-cultured with healthy peripheral blood mononuclear cells (PBMCs). The 12 cell lines were classified into Low and High-mels according to their inhibitory potential for IFN- α -pSTAT1 in co-culture PBMCs. Comparison of gene transcription and aCGH data was conducted on Low and High-mels. Data analysis identified *NOS1* as the candidate determinant of immune inhibitory function in Low-Mels. Differential expressed genes by IPA-analysis suggested down-regulation of IFN α signaling in Low-mels. ***Middle panel:*** Validation of *NOS1* as the factor for the inhibitory function of Low-Mels. Purified CD3+T-cells were co-cultured with Low-Mels in the presence of a NOS1 selective inhibitor (NPLA) compared a control group culture in the presence of no inhibition of the NOS2 selective inhibitor (1400W). Only NPLA reversed purified CD3+T-cells from Low-mels inhibition but not 1400W. ***Lower panel:*** The data from patients. Correlation of NOS1 expression levels in melanoma with PBMCs response to IFN- α in 9 melanoma patients and correlation of NOS1 expression levels in melanoma with outcome to immunotherapy by adoptive tumor infiltrating lymphocytes (TILs).



Supplemental Figure 1

The levels of IFN- α -pSTAT1 but not basal-pSTAT1 of PBMC was altered by melanoma cell lines

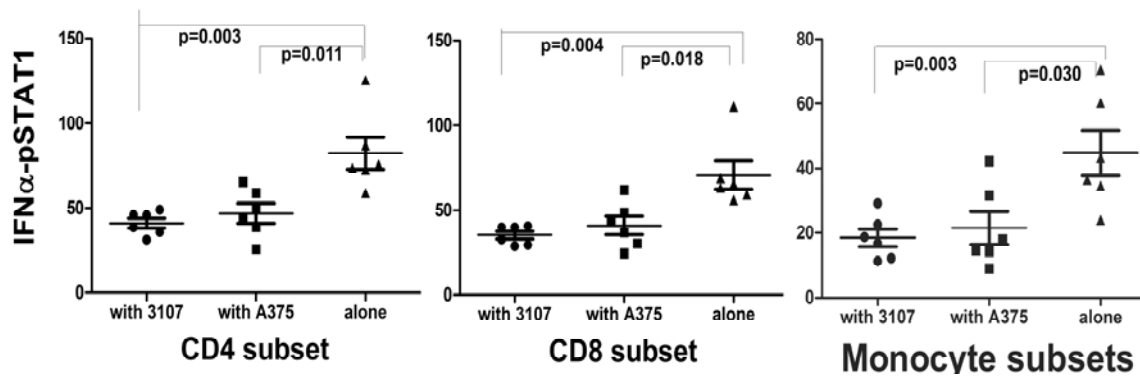
IFN- α -pSTAT1 in PBMCs subsets varied among co-cultured cell lines (P values = .0001, .0001 and .0009 for IFN- α -pSTAT1 in CD4⁺, CD8⁺ T, and monocytes subsets; Kruskal Wallis ANOVA), but not basal-pSTAT1 (P values = .46, .80, .99 for CD4⁺, CD8⁺ T, and monocytes subsets; Kruskal Wallis ANOVA);



Supplemental Figure 2

The basal-pSTAT1 but not IFN α -pSTAT1 of PBMC subsets varies among independent blood donors.

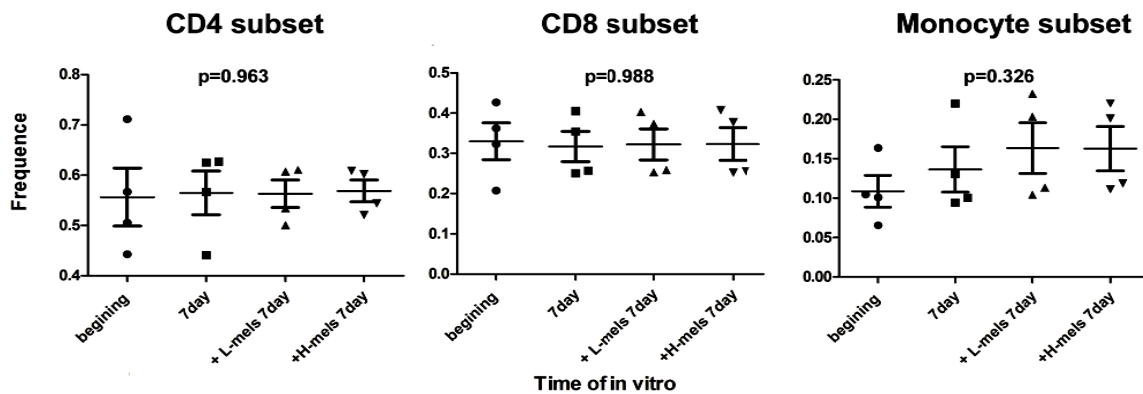
Basal-pSTAT1 in CD4⁺, CD8⁺ and monocytes subsets differed among 4 donors ($P = .0001$ all the three subsets), but IFN- α -pSTAT1 in CD4⁺ and CD8⁺ T cells not did ($P = .12, .13$) and IFN- α -pSTAT1 in monocytes varied mildly ($P = .03$, Kruskal-Wallis ANOVA).



Supplemental Figure3

Inhibition of PBMCs' IFN α -pSTAT1 levels by melanoma when maintained in autologous serum.

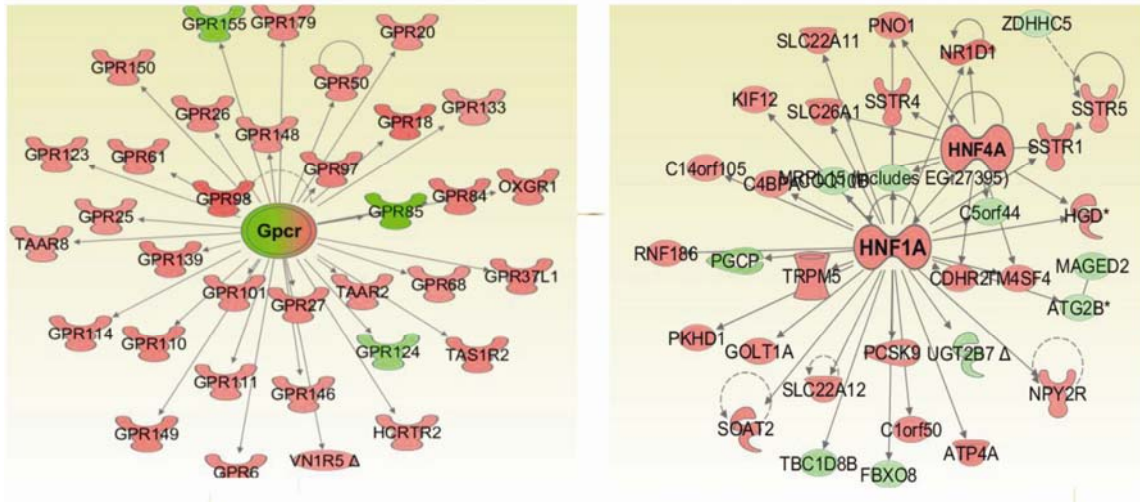
CD4⁺ (Left), CD8⁺ (Middle) T cells and monocytes (Right) co-cultured with L-mels of 3107 and A375 when maintained in autologous serum; comparable reduction of responsiveness to IFN- α stimulation was observed (Paired T test, p-values = 0.003, 0.011 for CD4⁺, 0.004, 0.018 for CD8⁺ and 0.003, 0.03 for monocyte subsets by 3107 and A375 respectively).



Supplemental Figure4

Frequency of PBMC subsets was not altered by co-culture with melanoma cells

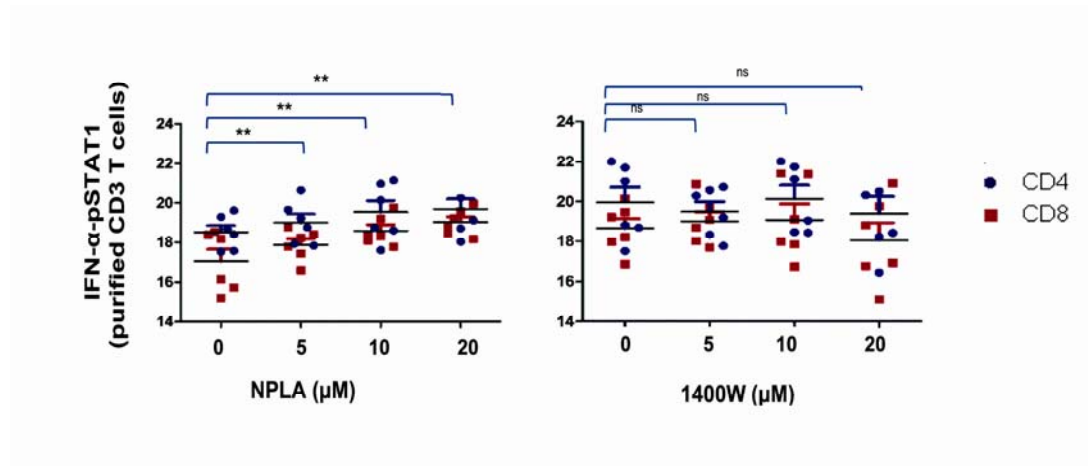
No significant changes were observed comparing starting conditions with frequencies after 7-day in vitro culture whether the PBMCs had been co-cultured with L-mels or alone (Kruskal Wallis ANOVA. P= 0.287, 0.955, 0.376 for CD4⁺, CD8⁺ and monocytes respectively)



Supplemental Figure5

Activity of G-protein coupled receptor/ STAT3 downstream signaling pathways in the L-mel-signature

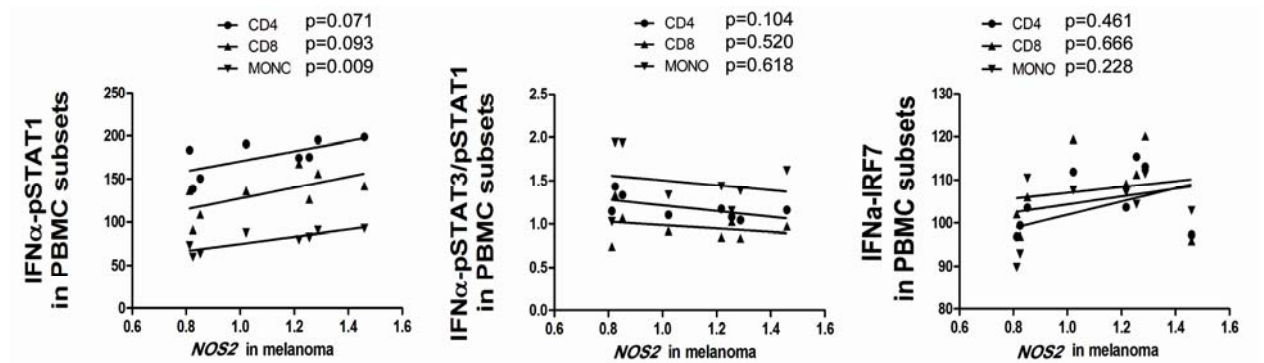
Up-regulation of G-coupled receptors (left) and downstream transcript factors (right) in the L-mel signature; analysis by IPA.



Supplemental Figure 6

Restoration of IFN- α -pSTAT1 levels in purified CD3⁺ T cells by NOS1 inhibitor but not NOS2 inhibitor

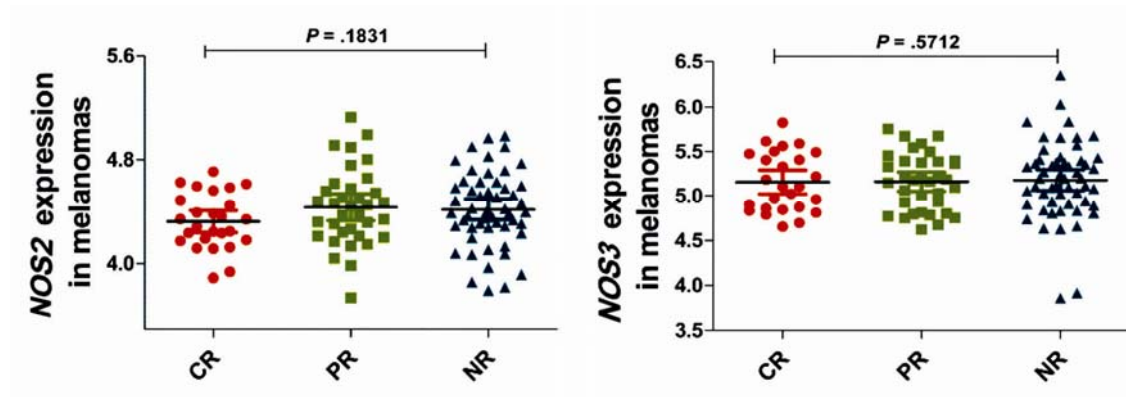
Suppression of IFN- α -pSTAT1 levels in purified CD3⁺ T cells was reversed by NPLA at minimal concentrations (5 μ M, 10 μ M, 20 μ M, $P = .0024, .0034, .0024$, **Left**). In contrast, the NOS2-specific inhibitor 1400W did not affect significantly IFN- α -pSTAT1 in the same conditions (**Right**).



Supplemental Figure 7

Analyzing the extent of correlation between IFN- α -pSTAT1 in PBMC subsets with in vivo NOS2 expression in paired melanoma metastases.

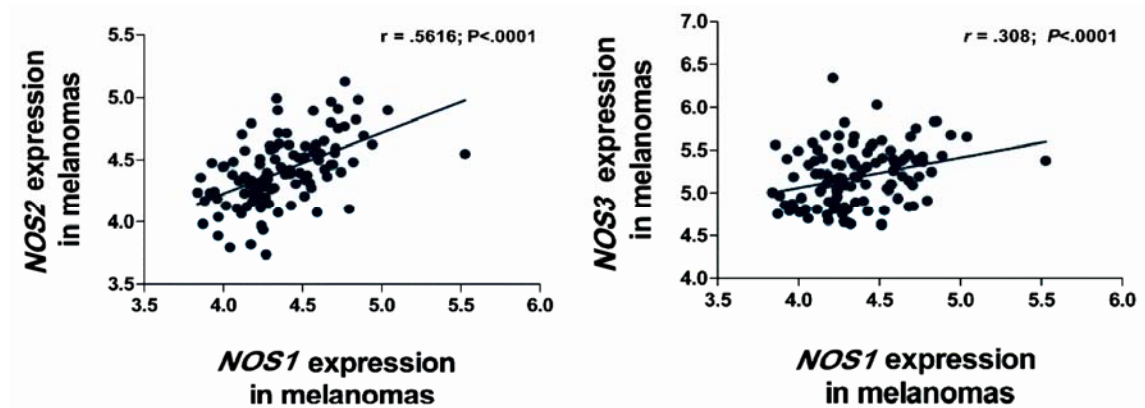
Left: *NOS2* expressions did not correlate with IFN- α -pSTAT1 in CD4⁺ and CD8⁺ subsets, but positively correlated in monocytes (Pearson r ; $p = 0.0706, 0, 0.0926, 0.0091$). No correlation between *NOS2* expression and IFN- α -pSTAT3/1 or IFN- α -pIRF7 in all three subsets ($p = 0.1044, 0.5197, 0.6175$ for IFN- α -pSTAT3/1; $p = 0.4597, 0.6657, 0.2282$ for IRF7 by CD4⁺, CD8⁺ and monocyte subsets respectively).



SupplementalFigure8

Expression of NOS2 and NOS3 in melanoma metastases did not correlate with the outcome of TIL therapy.

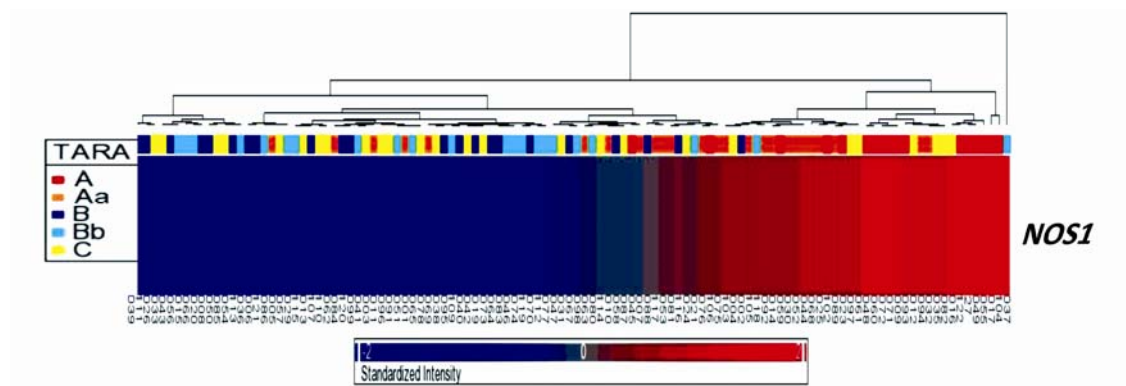
Expressions of *NOS2* (**Left**) and *NOS3* (**Right**) are not significantly different among 113 metastases from patients experiencing CR, PR, and NR following adoptive TIL therapy (CR = complete response, PR = partial response and NR = Non response (P = .1831 and .5712 for *NOS2* and *NOS3* respectively, one way ANOVA).



Supplemental Figure9

Correlating NOS1 expression to NOS2 and NOS3 in melanoma metastases

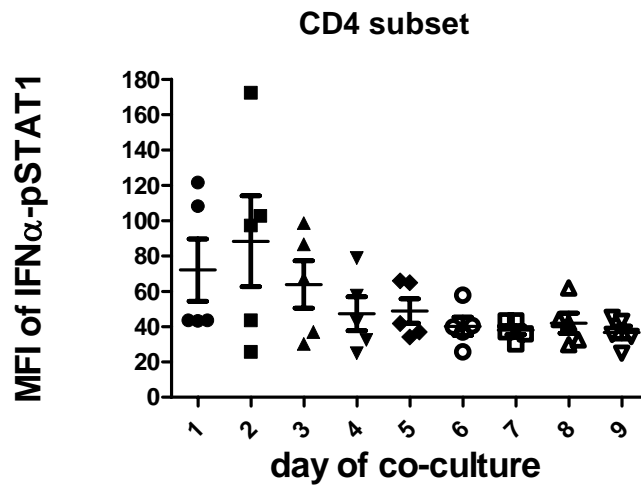
NOS1 expression was correlated with *NOS2* (*Left*) and *NOS3* (*Right*) ($r = 0.5616, 0.308$, $P = 0.0000, 0.0009$ for *NOS2* and *NOS3*, Spearman's correlation).



Supplemental Figure 10

***NOS1* expression in melanoma metastases correlates with TARA class.**

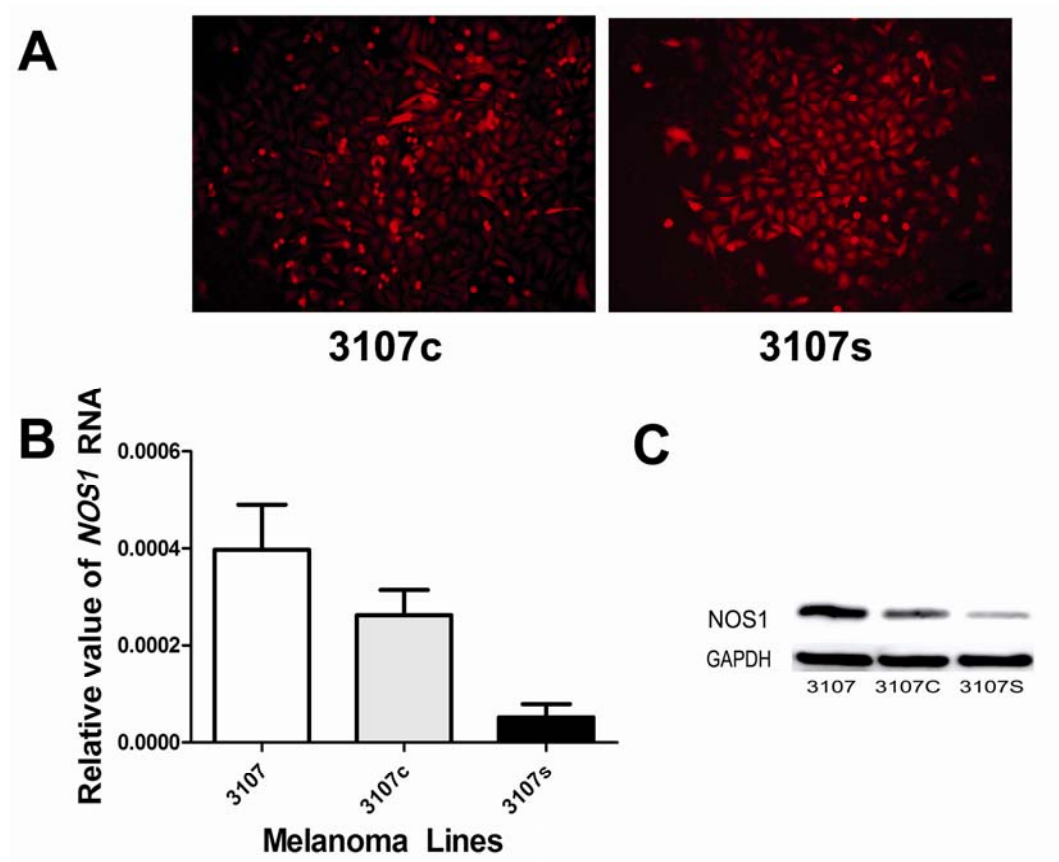
Melanoma metastases were characterized according to the recently described TARA classification (Spivey *et al.* BMC Genomics 2012). TARA class A and Aa corresponds to a poor prognosis cancer phenotype characterized by an enrichment of Th17 signature.



Supplemental Figure 11

Time course analysis of IFN α -pSTAT1 in CD4⁺ T cells when co-cultured with melanoma L-mel624

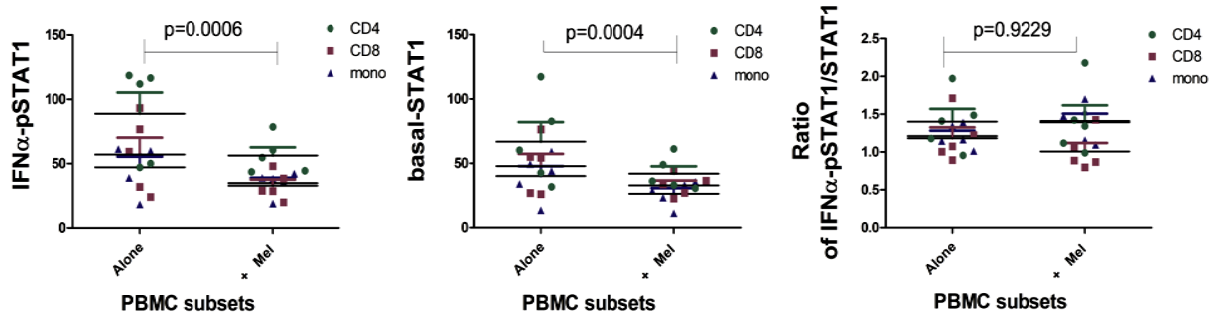
CD4⁺ T cells' STAT1 phosphorylation levels are shown (n=5) during co-culture with the melanoma cell line L-mel624.



Supplemental Figure12

Genetic knockdown of NOS1 in the strongly inhibitory L-mel 3107 cell line.

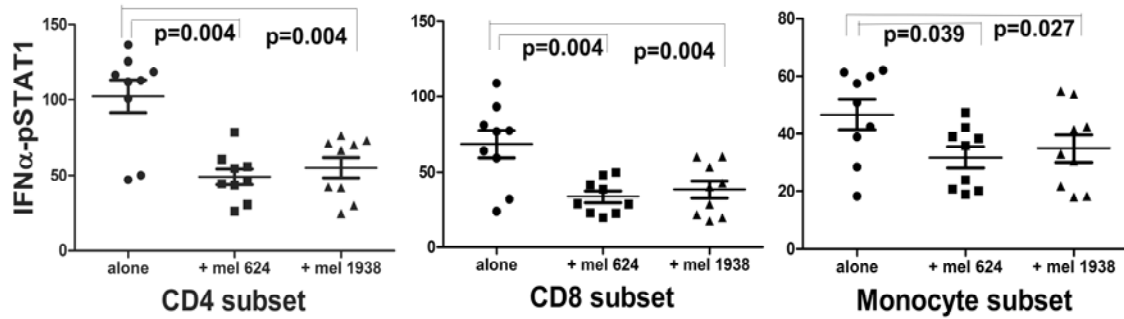
A) The image of NOS1 shRNA clone of L-mel 3107 (3107s) and its control clone (3107c). B). Relative value of *NOS1* RNA in 3107, 3107c and 3107s clones as assessed by real-time PCR. C) Western blotting image for NOS1 protein in 3107, 3107c and 3107s clones.



Supplemental Figure 13

Comparison of IFN α -pSTAT1 and basal-STAT1 protein levels and of IFN α -pSTAT1/STAT1 in PBMCs from five healthy donors

Comparisons were made between T cells co-cultured with L-mel 624 and alone. IFN α -STAT1 (left) and STAT1 (middle) in PBMCs subsets reduced significantly by co-culture with melanoma line 62428 (Paired t test, p=0.0006 and 0.0004, for IFN α -pSTAT1 and STAT1 respectively); but not in the ratio of IFN α -pSTAT1/STAT1 (Right, p=0.5229).



Supplemental Figure 14

Inhibitory role of melanoma cells on PBMCs' IFNα-pSTAT1 levels when analyzing CD4⁺, CD8⁺ and monocyte subsets separately.

Inhibition of IFNα-pSTAT1 in PBMCs subsets by L-mels also were significant when analyzed individually on CD4⁺ (Left), CD8⁺ (Middle), and monocytes (Right) subsets (Paired T test, p=0.004, 0.004 for CD4⁺, 0.004, 0.004 for CD8⁺ and 0.039, 0.027 for monocyte subsets by L-mel 62428 and 1938 respectively). (n=9)

2. Supplemental Tables:

Supplemental Table1

Transcription factors predicted to be inhibited in the L-melsignature (IPA, z –score <-2)

Transcription	Predicted	
Regulator	Activation State	Regulation z-score
XBP1 (includes		
EG:140614)	Inhibited	-5.045
TFEB	Inhibited	-3.383
IRF7	Inhibited	-3.253
Nfat (family)	Inhibited	-2.963
MITF	Inhibited	-2.92
IRF5	Inhibited	-2.668
NFE2L2	Inhibited	-2.487
PRDM1	Inhibited	-2.475
HIC1	Inhibited	-2.446
STAT1	Inhibited	-2.184
YY1	Inhibited	-2.177
E2F1	Inhibited	-2.159
STAT4	Inhibited	-2.15
SF1 (includes		
EG:15499)	Inhibited	-2.132

Supplemental Table2:

Predicted status of STAT3 targets in the L-melsignature (by IPA, z –score <-2)

Genes	Fold Change	Genes	Fold Change
TERT	1.755	TNFSF11	1.216
ISG20	1.727	NPPA	1.208
SALL4	1.702	NPY	1.208
IGF1R	1.515	POU5F1	1.194
CD40LG	1.402	LILRB4	1.193
ESR2	1.375	IL17F	1.193
C5AR1	1.372	REG1B	1.192
ALAS2	1.304	TBX21	1.18
APOA4	1.302	OMP	1.174
TRH	1.275	REN	1.159
LIF	1.264	FGA	1.157
IGFBP1	1.26	ITGB2	1.153
AGRP	1.258	CDH5	1.152
GFAP	1.253	HAMP	1.143
PIM3	1.251	ARG1	1.141
CCL4	1.249	CSN2	1.138
CEBPA	1.236	IL17A	1.125
LILRB2	1.233	CCR5	1.113
HNF4A	1.225	IL23R	1.11
GADD45G	1.225	IL23A	1.109
SFTPB	1.224	FGB	1.109
CCL17	1.224	FGG	1.106
CDKN2D	1.222	VIP	1.099
RORC	1.216		

Supplemental Table3:

The nineteen genes of the 12q24 segment showing both frequent chromosomal amplification and up-regulated gene expression in L-mel cell lines

Gene Symbols

B3GNT4

FOXN4

MORN3

SETD8

CABP1

GPR109B

NOS1

SRRM4

CDK2AP1

HNFB1A

OGFOD2

SUDS3

DNAH10

IL31

RNFT2

WSCD2

FAM101A

KSR2

SETD1B

Supplemental Table 4:

NOS1 copy number variation and mRNA levels in L-mel and H-mel cell lines

<i>Cell line Name</i>	<i>group</i>	<i>L-RNA</i>	<i>NOS1 Copy number</i>
<i>A375</i>	L-mels	6.16578	Amplification
<i>62428</i>	L-mels	6.16594	Amplification
<i>888</i>	L-mels	6.20363	Amplification
<i>938</i>	L-mels	6.10864	Amplification
<i>3107</i>	L-mels	6.19139	Amplification
<i>3104</i>	L-mels	5.98086	Unchanged
<i>146II</i>	L-mels	6.21428	Unchanged
<i>1858w</i>	L-mels	6.22958	Unchanged
<i>2224</i>	H-mels	5.95026	Unchanged
<i>2035</i>	H-mels	5.91202	Unchanged
<i>1858M</i>	H-mels	5.94316	Unchanged
<i>1290p14</i>	H-mels	5.68613	Unchanged
<i>1195</i>	H-mels	5.83637	Unchanged
<i>1866</i>	H-mels	5.79502	Unchanged
<i>1858F</i>	H-mels	5.89673	Deletion
<i>261IV</i>	H-mels	5.66674	Deletion
<i>1182</i>	H-mels	6.09607	Deletion
<i>2523</i>	H-mels	6.03419	Deletion

3. Supplemental Methods:

Clinical samples – detailed description

Samples 113 pre-treatment tumor biopsies were available for RNA extraction. Samples were collected during five consecutive trials at the Surgery Branch, National Cancer Institute (NCI) (Dudley *et al*, 2010; Rosenberg *et al*, 2011; Bedognetti *et al*, 2013) codified as: TNMA, T200, T1200, TYT, and TCD8. All patients had progressive disease and had previously received standard or experimental regimens. Fifty percent of the patients (71/142) achieved an objective response (OR), of which 25 (18%) experienced a durable complete response (CR) and 46 (32%) a partial response (PR). Tumor biopsy samples included 24 CR (21%), 34 PR (30%) and 55 (49%) non-response (NR) samples.

Two Gy or 12 Gy total body irradiation (TBI) was administered in conjunction with chemotherapy in T200 and T1200 trials, respectively (Rosenberg *et al*, 2011). A day following lymphodepletion, TILs were infused into patients and high-dose IL-2 therapy was started. Protocols employed to generate TILs are described elsewhere (Dudley *et al*, 2010; Dudley *et al*, 2003; Rosenberg *et al*, 2011; Tran *et al*, 2008). Before TIL administration, patients received a nonmyeloablativelymphodepleting regimen consisting of cyclophosphamide at 60 mg/Kg/d for 2 days and fludarabine at 25 mg/m²/d for 5 days (Dudley *et al*, 2010; Rosenberg *et al*, 2011). A day following lymphodepletion, TILs were infused into patients and high-dose IL-2 therapy was started (720,000 IU/Kg intravenously every 8 hours to tolerance). Major inclusion criteria included minimum age of 18 years, measurable disease, good clinical performance and life expectancy greater than 3 months. Detailed study protocols information are available elsewhere (<http://clinicaltrials.gov/ct2/show/NCT00513604?term=07C0176&rank=1>), (Dudley *et al*, 2010; Rosenberg *et al*, 2011). All patients signed an informed consent approved by the Institutional Review Board of the NCI. Data for this analysis are updated as of January 11,

2012. Response (CR, PR, or NR) was rated according to Response Evaluation Criteria in Solid Tumors (RECIST) guidelines 4 weeks following TIL administration and at regular intervals thereafter. A CR or PR was considered an OR and a PR or NR was considered a Non-CR.

Gene expression analysis. Total RNA was isolated from 142 TILs (cryopreserved just before the infusion into the patients) and 113 snap frozen tumor samples used for TIL generation. Total RNA was extracted with the QiagenmiRNeasy Mini kit and its quality tested with the Agilent Bioanalyzer 2000 (Agilent Technologies, Palo Alto, CA). Three hundred ng of total RNA was used for RNA amplification according to manufacturer's instructions (WT Expression Kit; Ambion, Austin, TX). aRNA were reverse transcribed into cDNAs followed by fragmentation. After hybridization to the GeneChip Human Gene 1.0 ST Arrays, the chips were labeled with a WT Terminal Labeling Kit (Affymetrix, Santa Clara, CA) and scanned on a GeneChip Scanner 3000 7G (Affymetrix, Santa Clara, CA). Data were normalized using the Robust Multi-Chip Average (RMA) method and Log_2 transformed using Partek Genomics Suite 6.4 (Partek Inc., St. Louis, MO). Data analyses were based on the whole transcripts.

Statistical analysis. See in the manuscript.